



Vibrational frequencies of hydrogenated silicon carbonitride: A DFT study

Romain Coustel, Mathias Haacké, V. Rouessac, Erwan André, Stephanie Roualdes, Anne Julbe

► To cite this version:

Romain Coustel, Mathias Haacké, V. Rouessac, Erwan André, Stephanie Roualdes, et al.. Vibrational frequencies of hydrogenated silicon carbonitride: A DFT study. Surface and Coatings Technology, 2017, 325, pp.437 - 444. 10.1016/j.surfcoat.2017.06.017 . hal-01675264

HAL Id: hal-01675264

<https://hal.umontpellier.fr/hal-01675264>

Submitted on 3 Dec 2022

HAL is a multi-disciplinary open access archive for the deposit and dissemination of scientific research documents, whether they are published or not. The documents may come from teaching and research institutions in France or abroad, or from public or private research centers.

L'archive ouverte pluridisciplinaire **HAL**, est destinée au dépôt et à la diffusion de documents scientifiques de niveau recherche, publiés ou non, émanant des établissements d'enseignement et de recherche français ou étrangers, des laboratoires publics ou privés.

Vibrational frequencies of hydrogenated silicon carbonitride: A DFT study

Romain Coustel ^{a,*}, M. Haacké ^b, V. Rouessac ^b, E. André ^a, S. Roualdès ^b, A. Julbe ^b

^a Université de Lorraine, Laboratoire de Chimie Physique et Microbiologie pour l'Environnement, LCPME, UMR 7564, Villers-lès-Nancy F-54600, France

^b Institut Européen des Membranes, UMR 5635 CNRS-UM2-ENSCM, Université de Montpellier (cc 047), 34095 Montpellier cedex 5, France

* romain.coustel@univ-lorraine.fr

Due to their good chemical and thermal inertness, SiC_xN_y:H films are suitable for a variety of applications in electronic, tribology, optic, photovoltaic and more recently gas separation membranes. For these applications, film evolution can be attractively probed by FTIR spectroscopy. In this work, a systematic quantum mechanical study of the vibrational modes position in the pattern of a-SiC_xN_y(O):H is presented. Vibrational frequencies of Si—C, Si—N, C≡N, Si—H, C—H and N—H moieties have been calculated at DFT/B3LYP level of theory using the 6-311++G(3df,3pd) basis set. Characteristic absorption domains have been compared with FTIR data from the literature. In particular, DFT calculations provide guidelines to discriminate Si—H from C≡N stretching bands, which are calculated to lie below and above ~2230 cm⁻¹, respectively. As an example, the oxidation of a microwave PECVD SiC_xN_y:H films during ageing was evidenced in this work through the progressive increase of Si—O stretching band (~1040 cm⁻¹). The simultaneous decay of the band centered at 2170 cm⁻¹ was attributed to the vanishing of Si—H bond upon oxidation. This example illustrates that unambiguous band assignment is required to provide a molecular description of the ageing process, which is in turn required to optimize the material composition and stability. Results of these calculations will be helpful to identify both the chemical moieties and their environment in future investigations on a-SiC_xN_y:H materials but also on materials containing additional elements such as B- or O-doped SiCN-based systems.

1. Introduction

Amorphous hydrogenated silicon carbonitride films have been subject of significant research effort over the past decade [1–28]. Indeed, SiC_xN_y:H appears as a promising candidate for a wide range of applications including mechanical layer [6,8,10,20,21,23,24], optical layer [1,3,6,9,18–22,25], low-k dielectric layer [4,5], protective layer [17,20], surface passivation layer for silicon solar cells [2,7,25] and gas separation membranes [13,26–28].

Amorphous silicon carbonitride films have been obtained through various deposition techniques including both physical vapor deposition (PVD) and chemical vapor deposition (CVD). In particular, different magnetron PVD technologies (DC [17,24] RF [17,18] or high power pulse magnetron sputtering [17]), as well as vapor transport-CVD [16] or different plasma enhanced CVD (PECVD) technologies (low frequency [13,23,25–27], radio frequency [2,4–9,12,14,15], microwave, [1,19,22,28] remote PECVD [3,10,11] or atmospheric pressure PECVD [20,21]), were carefully examined in the literature. Adjusting the deposition conditions (type and concentration of precursor, additional reactants,

substrate temperature, type of carrier gas...) allows tuning both the composition and the bonding configuration that greatly affect material properties (electronic properties [22], gas transport [26], ...). This versatility is a unique feature of SiC_xN_y:H materials. Within this framework, Fourier Transform Infrared (FTIR) spectroscopy is a convenient and powerful tool to probe the material bond structure.

Fig. 1 provides a review (reference numbers are given on x-axis) of the FTIR absorption bands positions given in the literature for such films. They are characterized in mid infrared by a broad absorption band between 600 and 1300 cm⁻¹, which results from the overlap of several peaks attributed to Si—H wagging, Si—C and Si—N stretching, CH₂ wagging, N—H bending and Si—CH₃ symmetric deformation. The absorption band in the range 2000–2300 cm⁻¹ is attributed to Si—H or C≡N stretching modes, depending on authors. Bands at about 2950 and 3400 cm⁻¹ are assigned to C—H stretching and N—H stretching, respectively. Surprisingly, as already noted by Peter et al. [23], the published peak positions might vary by 150 cm⁻¹ and more (Fig. 1).

The presence of additional elements such as boron or oxygen makes FT-IR spectra interpretation even more difficult. In order to further tune the properties of SiCN films, boron doping was investigated. Corresponding FTIR spectra shows extra absorption bands contributing in the 700–1400 cm⁻¹ region (see for example ref. [29]). Hydrogenated

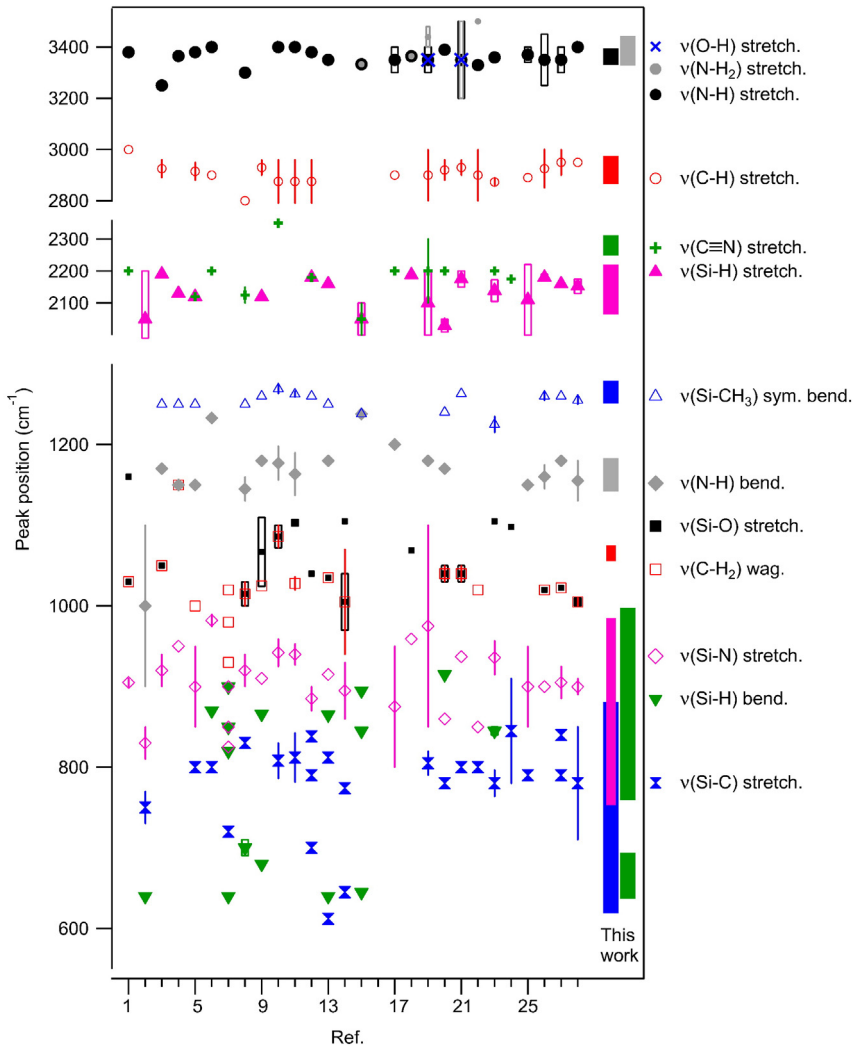


Fig. 1. Comparison of peak positions or ranges of absorption reported in the literature for $\text{SiC}_x\text{N}_y(\text{O}):\text{H}$ films (reference numbers are given on x-axis). The values calculated in the present work are also reported for comparison.

silicon carbonitride films commonly present oxygen contamination (evidenced by X-ray photoemission spectroscopy), while strong Si—O stretching band is located close to $1000\text{--}1200\text{ cm}^{-1}$ (Fig. 1). Even if high chemical and thermal inertness make $\text{SiC}_x\text{N}_y:\text{H}$ material suitable for a large number of applications in aggressive environment (passivation layer, tribological application, gas separation membrane...), film evolution can be attractively probed by FTIR spectroscopy. The oxidation of microwave PECVD $\text{SiC}_x\text{N}_y:\text{H}$ films during ageing was evidenced through the progressive increase of Si—O stretching band ($\sim 1040\text{ cm}^{-1}$). The simultaneous decay of the band centered at 2170 cm^{-1} was attributed to the vanishing of Si—H bond upon oxidation [28]. This example illustrates that unambiguous band assignment is also required to provide a molecular description of the ageing process, which is in turn required to optimize film stability.

In order to rationalize the vibrational properties of silicon containing materials, much attention was paid to silica or $\text{SiO}_x\text{C}_y:\text{H}$ materials through either experimental or theoretical studies [30–33]. Simple organosilicon compounds have also been studied at the density functional theory (DFT) level [32,34–36] as well as the Si—H stretching frequency in microcrystalline Si_xH_y [37]. However a systematic DFT study of the vibration frequencies of a- $\text{SiC}_x\text{N}_y(\text{O}):\text{H}$ system is still missing. This is the purpose of the present work that focuses on the calculation of the vibrational frequencies associated to Si—C, Si—N, C≡N, Si—H, C—H and N—H bonds. In order to remain concise, other types of chemical moieties such as C—C, C=C, C—N, C=N... which are scarcely

expected to form in Si rich silicon carbonitride materials have not been considered in the present work. The discussion about calculated frequencies focuses on two main issues: (i) the wide dispersion of the frequencies reported in literature and (ii) the ambiguity between Si—H and C≡N stretching bands. Comparison between experimental and theoretical data highlights the effect of chemical environment on the position of the considered vibrational modes in hydrogenated silicon carbonitride. Eventually, the presented results are also sound for the analysis of B- or O-doped SiCN-based system.

2. Computational details

Calculations were performed at the DFT level of theory using the Becke three-parameter exchange functional [38], along with the Lee-Yang-Parr [39] gradient-corrected correlation functional [the so-called Becke three-parameter Lee-Yang-Parr (B3LYP) functional] as implemented in the GAMESS software program package [40]. Model compounds containing Si—H, C—H, N—H, Si—C, Si—N or C≡N bond were considered in order to evaluate the vibrational properties of a- $\text{SiC}_x\text{N}_y(\text{O}):\text{H}$ materials. After geometry optimizations, vibrational frequencies were calculated from the Hessian matrix. The bond of interest as well as the nearest neighbor atoms were described by using the 6-311++G(3df,3pd) basis set. In order to save calculation time, (i) SBKJC core effective potentials were used for other atoms and (ii) these atoms were kept frozen for Hessian matrix calculations. It has

been checked that (i) and (ii) does not significantly affect vibrational frequencies calculations. For example, $\nu(\text{Si—H stretch.})$ in $\text{HSiSi}_3(\text{Si}^{\text{a}}\text{H}_3)_9$ is downshifted by only 4 cm^{-1} when all Si^{a} atoms are unfrozen and described with the $6\text{-}311++\text{G}(3\text{df},3\text{pd})$ basis set.

In order to take into account the anharmonic effects on vibrational frequencies, the correlation corrected vibrational self-consistent field (cc-VSCF) approach was used within the quartic force field (QFF) approximation [41]. In order to save calculation time, anharmonic frequencies were computed only for representative compounds, from which scale factors were evaluated. For instance, the vibration frequencies of both Si—H and C≡N bonds have been considered in various chemical environments. As shown in Table 1, anharmonic effect has been found to be systematically more pronounced for Si—H than for C≡N stretching mode. From anharmonic/harmonic frequencies ratio, scale factors of 0.96 and 0.99, respectively, has been retained. Determined scale factors (Table 2) are in line with the recommendation given by Merrick et al. [42] for B3LYP/6-311++G(3df,3pd) level of theory.

3. Results and discussion

For simplification purpose, band positions are discussed in the order of increasing wavenumbers in the mid-infrared region. Note also that, for the sake of brevity, when vibrational frequency is discussed vs. chemical environment of the considered bond, only the nearest neighbor atoms are indicated in the text, i.e. $\nu(\text{Si—H stretch.})$ in HSiSi_3 is calculated for $\text{HSiSi}_3(\text{SiH}_3)_9$. The complete formulas of all the compounds that have been considered for calculations are reported in Table 2.

3.1. Si—C stretching/Si—N stretching

The main contributions to the broad adsorption band of $\text{a-SiC}_x\text{N}_y\text{:H(O)}$ films, ranging from 600 to 1300 cm^{-1} , come from Si—C and Si—N stretching modes. The Si—C stretching absorption band was reported to lie in the range $612\text{--}910\text{ cm}^{-1}$ (Fig. 1 and reference herein). Calculated wavenumbers for various chemical environments of the Si—C bond are detailed in Table 2. Simulated $\nu(\text{Si—C stretch.})$ appears to spread over the range $619\text{--}881\text{ cm}^{-1}$, which correctly reproduces the distribution of experimental results. It appears that the position of $\nu(\text{Si—C stretch.})$ band decreases when switching from $\text{Si}_3\text{C—SiX}_3$ to $\text{H}_2\text{C—(SiX}_3)_2$, to $\text{H}_3\text{C—SiX}_3$ (with $\text{X} = \text{Si, C, N, O}$) and to $(\text{H}_3\text{C})_x\text{—Si—Si}_{4-x}$ (with $x = 1\text{--}3$). Such a trend reveals that the H concentration in the film should greatly affect the low wavenumber side of the Si—C stretching component. In addition, a slight shift of $\nu(\text{Si—C stretch.})$ toward higher wavenumbers has to be anticipated for materials with an increasing amount of electronegative atoms. As an example, $\nu(\text{Si—C stretch.})$ in $\text{Si}_3\text{C—SiX}_3$ increases from 792 to 881 cm^{-1} when $\text{X} = \text{Si}$ is replaced by O.

Similar results are obtained for $\nu(\text{Si—N stretch.})$ (Table 2). Indeed, $\nu(\text{Si—N stretch.})$ decreases in the series from $\text{Si}_2\text{N—SiX}_3$ to $\text{HN—(SiX}_3)_2$ and to $\text{H}_2\text{N—SiX}_3$, and electronegative atoms in the

vicinity of Si—N bond induce absorption band shift toward higher wavenumbers. Calculations give $\nu(\text{Si—N stretch.})$ in the range $804\text{--}985\text{ cm}^{-1}$, in good agreement with the reported experimental values which lies in the range $800\text{--}1100\text{ cm}^{-1}$, with most of them in the range $830\text{--}960\text{ cm}^{-1}$ (Fig. 1). The absence of any reported absorption below 800 cm^{-1} should be attributed to the missing $(\text{H}_2\text{N})_2\text{—Si}$ or $(\text{H}_2\text{N})_3\text{—Si}$ moieties, in agreement with the chemical structure of the precursors used for preparing the $\text{SiC}_x\text{N}_y\text{:H(O)}$ films. For example, the lowest position for $\nu(\text{Si—N stretch.})$ is calculated for the $(\text{H}_2\text{N})_3\text{—Si}$ moiety which is not present in the common N containing precursors used in the literature (typically N_2 , NH_3 , or $\text{NH}[\text{Si}(\text{CH}_3)_3]_2$) and is thus not expected in the derived PECVD materials.

3.2. Si—H bending

FTIR investigations report two absorption bands located at $640\text{--}710\text{ cm}^{-1}$ and $820\text{--}915\text{ cm}^{-1}$ corresponding to Si—H deformation modes (Fig. 1 and reference herein). Calculations for $\text{X}_3\text{—SiH}$, $\text{X}_2\text{—SiH}_2$ and X—SiH_3 ($\text{X} = \text{Si, C, N or O}$) moieties sustain this assignment (Table 2). The calculated bending wavenumbers can be divided into two subgroups at $637\text{--}694\text{ cm}^{-1}$ and $759\text{--}998\text{ cm}^{-1}$. The former is obtained for $\text{Si}_3\text{—SiH}$ moieties, while higher wavenumbers correspond to more electronegative environments ($\text{X} = \text{C, N or O}$) of Si—H. Then, low $\nu(\text{Si—H bend.})$ wavenumbers are expected for Si-rich materials. One should note that relatively low $\nu(\text{Si—H bend.})$ in $\text{Si}_3\text{—SiH}$ is correlated to the relative weakness of the Si—H bond (e.g. $d(\text{Si—H}) = 1.492\text{ \AA}$, 1.487 \AA , 1.480 \AA and 1.463 \AA in $\text{X}_3\text{—SiH}$, with $\text{X} = \text{Si, C, N or O}$ respectively).

3.3. CH₂ wagging

DFT calculations indicate that CH_2 -wagging modes in $(\text{X}_3\text{Si})_2\text{—CH}_2$ ($\text{X} = \text{Si, C, N, O}$) are gathered in the narrow range $1055\text{--}1075\text{ cm}^{-1}$ (Table 2). In experimental studies, CH_2 -wagging wavenumbers are generally widely dispersed in the range $930\text{--}1150\text{ cm}^{-1}$. This discrepancy suggests that the CH_2 contribution can hardly be isolated due to overlapping/coupling of absorption band in this region (namely Si—N, Si—O and C—N stretching modes). For example, the C—N stretching mode in $\text{Si}_3\text{—CN—Si}_2$ was calculated to appear at 985 cm^{-1} (unscaled).

3.4. N—H bending

Contrary to the CH_2 wagging modes, the N—H bending mode is clearly identified in FTIR spectra: it is reported to lie in the range $900\text{--}1240\text{ cm}^{-1}$ and more precisely in the range $1130\text{--}1200\text{ cm}^{-1}$ for a vast majority of studies. DFT results are consistent with this latter narrow range: wavenumbers calculated for $(\text{X}_3\text{Si})_2\text{—NH}$ ($\text{X} = \text{Si, C, N or O}$) are in between 1142 and 1183 cm^{-1} . Then, published result corresponding to a much more extended absorption range should be considered with caution.

3.5. Si—CH₃ symmetric bending

The C—H symmetric bending mode in Si—CH_3 appears as a narrow absorption band centered at $1240\text{--}1275\text{ cm}^{-1}$ depending on studies. Our calculations for $\text{H}_3\text{C—SiX}_3$ ($\text{X} = \text{Si, C, N or O}$) moieties give a restricted range of vibrations (Table 2) with $\nu(\text{C—H}_3\text{ sym. bend.})$ in between 1267 and 1279 cm^{-1} . Vibrational coupling between CH_3 groups (in $(\text{H}_3\text{C})_x\text{—Si—Si}_{4-x}$) slightly extends this range up to $1251\text{--}1279\text{ cm}^{-1}$.

3.6. Si—H stretching

Special attention was paid to the Si—H stretching vibration mode. It is well known that this frequency strongly depends on the Si chemical environment. In early works on organosilicon compounds [43] and Si-

Table 1

Harmonic and anharmonic frequencies of Si—H and C≡N stretching modes for different moieties.

Vibrational mode	Moiety	ν_h harmonic frequency (Hessian) (cm^{-1})	ν_a anharmonic frequency (cc-VSCF/QFF) (cm^{-1})	ν_a/ν_h	
Si—H stretch.	HSi(OSiH ₃) ₃	2314	2224	0.96	
		CH ₃ SiH ₃	2217	2133	0.96
			2215	2114	0.96
			2215	2107	0.95
	NH ₂ SiH ₃	2230	2129	0.96	
		2228	2141	0.96	
		2175	2079	0.96	
		C≡N stretch.	NCSiH ₃	2309	2278
NCSi(OSiH ₃) ₃	2315		2282	0.99	

Table 2

Calculated (DFT B3LYP/6-311++G(3df,3pd) level of theory) vibrational wavenumbers for Si—C, Si—N, C≡N, Si—H, C—H and N—H moieties.

$\nu(\text{Si-C stretch.}) (\text{cm}^{-1})$ Unscaled									
$(\text{H}_3\text{Si})_3\text{C-Si}(\text{SiH}_3)_3$	792	$\text{H}_2\text{C-Si}(\text{SiH}_3)_3$	765	$\text{H}_3\text{C-Si}(\text{SiH}_3)_3$	681	$(\text{H}_3\text{C})_2\text{-Si}(\text{SiH}_3)_2$	693-650		
$(\text{H}_3\text{Si})_3\text{C-Si}(\text{CH}_3)_3$	812	$\text{H}_2\text{C-Si}(\text{CH}_3)_3$	777	$\text{H}_3\text{C-Si}(\text{CH}_3)_3$	691	$(\text{H}_3\text{C})_3\text{-SiSiH}_3$	691-619		
$(\text{H}_3\text{Si})_3\text{C-Si}(\text{NH}_2)_3$	833	$\text{H}_2\text{C-Si}(\text{NH}_2)_3$	773	$\text{H}_3\text{C-Si}(\text{NH}_2)_3$	700				
$(\text{H}_3\text{Si})_3\text{C-Si}(\text{OH})_3$	881	$\text{H}_2\text{C-Si}(\text{OH})_3$	794	$\text{H}_3\text{C-Si}(\text{OH})_3$	748				
$\nu(\text{Si-N stretch.}) (\text{cm}^{-1})$ Unscaled									
$(\text{H}_3\text{Si})_2\text{N-Si}(\text{SiH}_3)_3$	912	$\text{HN-Si}(\text{SiH}_3)_3$	916	$\text{H}_2\text{N-Si}(\text{SiH}_3)_3$	810	$(\text{H}_2\text{N})_2\text{-Si}(\text{SiH}_3)_2$	863-783		
$(\text{H}_3\text{Si})_2\text{N-Si}(\text{CH}_3)_3$	941	$\text{HN-Si}(\text{CH}_3)_3$	938	$\text{H}_2\text{N-Si}(\text{CH}_3)_3$	804	$(\text{H}_2\text{N})_3\text{-SiSiH}_3$	909-753		
$(\text{H}_3\text{Si})_2\text{N-Si}(\text{NH}_2)_3$	949	$\text{HN-Si}(\text{NH}_2)_3$	936	$\text{H}_2\text{N-Si}(\text{NH}_2)_3$	847				
$(\text{H}_3\text{Si})_2\text{N-Si}(\text{OH})_3$	985	$\text{HN-Si}(\text{OH})_3$	959	$\text{H}_2\text{N-Si}(\text{OH})_3$	979				
$\nu(\text{Si-H stretch.}) (\text{cm}^{-1})$									
	Unscaled	Scaled (0.96)	Exp. [46,47,49-50]		Unscaled	Scaled (0.96)	Exp. [47-50]		
$\text{HSiSi}_3(\text{SiH}_3)_9$	2151	2065	2090/2000/2005/2013	$\text{H}_2\text{SiSi}_2(\text{SiH}_3)_6$	2189, 2181	2101, 2094	2116/2060/2065		
$\text{HSiSi}_2\text{C}(\text{SiH}_3)_9$	2159	2073	2054	$\text{H}_2\text{SiC}_2(\text{SiH}_3)_6$	2197, 2196	2109, 2108	2149		
$\text{HSiSiC}_2(\text{SiH}_3)_9$	2163	2076	2095	$\text{H}_2\text{SiN}_2(\text{SiH}_3)_4$	2222, 2211	2133, 2123	2170/2190/2175		
$\text{HSiC}_3(\text{SiH}_3)_9$	2177	2090	2135	$\text{H}_2\text{SiO}_2(\text{SiH}_3)_2$	2242, 2235	2152, 2146			
$\text{HSiSi}_2\text{N}(\text{SiH}_3)_8$	2170	2083	2100/2082	$\text{H}_3\text{SiSi}(\text{SiH}_3)_3$	2205, 2205, 2195	2117, 2117, 2107			
$\text{HSiSiN}_2(\text{SiH}_3)_7$	2178	2091	2140	$\text{H}_2\text{SiC}(\text{SiH}_3)_3$	2224, 2222, 2219	2135, 2133, 2130	2134		
$\text{HSiN}_3(\text{SiH}_3)_6$	2213	2124	2220/2160	$\text{H}_3\text{SiN}(\text{SiH}_3)_2$	2221, 2215, 2208	2132, 2126, 2120			
				$\text{H}_3\text{SiOSiH}_3$	2240, 2217, 2212	2150, 2128, 2124			
$\text{HSiSi}_2\text{O}(\text{SiH}_3)_7$	2165	2078	2134		Unscaled	Scaled (0.96)	Unscaled	Scaled (0.96)	
$\text{HSiSiO}_2(\text{SiH}_3)_5$	2211	2123	2195	$(\text{SiH}_3)_2\text{Si=SiHSi}(\text{SiH}_3)_3$	2206	2118	$\text{H}_2\text{Si=Si}(\text{SiH}_3)_2$	2262,2237	2172,2148
$\text{HSiO}_3(\text{SiH}_3)_3$	2314	2221	2248	$(\text{SiH}_3)_2\text{C=SiHC}(\text{SiH}_3)_3$	2244	2154	$\text{H}_2\text{Si=C}(\text{SiH}_3)_2$	2271,2249	2180,2159
$\text{HSiC}_2\text{N}(\text{SiH}_3)_8$	2177	2090		$(\text{SiH}_3)_2\text{N=SiHN}(\text{SiH}_3)_2$	2277	2186	$\text{H}_2\text{Si=N}(\text{SiH}_3)$	2255,2211	2165,2123
$\text{HSiCN}_2(\text{SiH}_3)_7$	2186	2099		$\text{O=SiHO}(\text{SiH}_3)$	2295	2203			
$\text{HSiCNO}(\text{SiH}_3)_6$	2191	2103							
$\nu(\text{C}\equiv\text{N stretch.}) (\text{cm}^{-1})$									
	Unscaled	Scaled (0.99)			Unscaled	Scaled (0.99)			
$\text{NCSiSi}_3(\text{SiH}_3)_9$	2272	2249		$\text{NCC}(\text{CH}_3)_3$	2335	2312			
$\text{NCSiC}_3(\text{SiH}_3)_9$	2295	2272							
$\text{NCSiN}_3(\text{SiH}_3)_6$	2301	2278							
$\text{NCSiO}_3(\text{SiH}_3)_3$	2315	2292							
$\nu(\text{C-H stretch.}) (\text{cm}^{-1})$					$\nu(\text{N-H stretch.}) (\text{cm}^{-1})$				
	Unscaled	Scaled (0.96)	Unscaled	Scaled (0.96)		Unscaled	Scaled (0.97)	Unscaled	Scaled (0.97)
$\text{H}_2\text{C}[\text{Si}(\text{SiH}_3)_2]_2$	3044	2922	$\text{H}_3\text{CSi}(\text{SiH}_3)_3$	3089	$\text{HN}[\text{Si}(\text{SiH}_3)_2]_2$	3544	3438	$\text{H}_2\text{NSi}(\text{SiH}_3)_3$	3626
	3001	2881		2964					3517
				3016					3434
				2895					
$\text{H}_2\text{C}[\text{Si}(\text{CH}_3)_2]_2$	3024	2903	$\text{H}_3\text{CSi}(\text{CH}_3)_3$	3075	$\text{HN}[\text{Si}(\text{CH}_3)_2]_2$	3549	3443	$\text{H}_2\text{NSi}(\text{CH}_3)_3$	3638
	2984	2865		2952					3529
				2907					3447
				2887					
$\text{H}_2\text{C}[\text{Si}(\text{NH}_2)_2]_2$	3049	2927	$\text{H}_3\text{CSi}(\text{NH}_2)_3$	3090	$\text{HN}[\text{Si}(\text{NH}_2)_2]_2$	3575	3468	$\text{H}_2\text{NSi}(\text{NH}_2)_3$	3652
	3004	2884		3071					3542
				2948					3456
				3009					
				2889					
$\text{H}_2\text{C}[\text{Si}(\text{OH})_2]_2$	3084	2961	$\text{H}_3\text{CSi}(\text{OH})_3$	3098	$\text{HN}[\text{Si}(\text{OH})_2]_2$	3612	3504	$\text{H}_2\text{NSi}(\text{OH})_3$	3664
	3033	2912		2974					3554
				2965					3468
				2901					
$\nu(\text{Si-H bend.}) (\text{cm}^{-1})$				$\nu(\text{SiH}_2\text{ wag.}) (\text{cm}^{-1})$			$\nu(\text{SiH}_3\text{ sym. bend.}) (\text{cm}^{-1})$		
	Unscaled				Unscaled	Scaled (0.99)		Unscaled	Scaled (0.99)
$\text{HSiSi}_3(\text{SiH}_3)_9$	637, 694		$\text{H}_2\text{SiSi}_2(\text{SiH}_3)_6$	767	759	$\text{H}_3\text{SiSi}(\text{SiH}_3)_3$	930	921	
$\text{HSiC}_3(\text{SiH}_3)_9$	863, 913		$\text{H}_2\text{SiC}_2(\text{SiH}_3)_6$	946	937	$\text{H}_3\text{SiC}(\text{SiH}_3)_3$	950	941	
$\text{HSiN}_3(\text{SiH}_3)_6$	879, 916		$\text{H}_2\text{SiN}_2(\text{SiH}_3)_4$	937	928	$\text{H}_3\text{SiN}(\text{SiH}_3)_2$	1008	998	
$\text{HSiO}_3(\text{SiH}_3)_3$	899, 900		$\text{H}_2\text{SiO}_2(\text{SiH}_3)_2$	959	949	$\text{H}_3\text{SiOSiH}_3$	1002	992	
$\nu(\text{CH}_2\text{ wag.}) (\text{cm}^{-1})$				$\nu(\text{CH}_3\text{ sym. bend.}) (\text{cm}^{-1})$			$\nu(\text{NH bend.}) (\text{cm}^{-1})$		
	Unscaled	Scaled (0.98)			Unscaled	Scaled (0.98)		Unscaled	Scaled (0.97)
$\text{H}_2\text{C}[\text{Si}(\text{SiH}_3)_2]_2$	1097	1075	$\text{H}_3\text{CSi}(\text{SiH}_3)_3$	1294	1268	$\text{HN}[\text{Si}(\text{SiH}_3)_2]_2$	1220	1183	
$\text{H}_2\text{C}[\text{Si}(\text{CH}_3)_2]_2$	1084	1062	$(\text{H}_3\text{C})_2\text{Si}(\text{SiH}_3)_2$	1295-1277	1269-1251	$\text{HN}[\text{Si}(\text{CH}_3)_2]_2$	1213	1177	
$\text{H}_2\text{C}[\text{Si}(\text{NH}_2)_2]_2$	1077	1055	$(\text{H}_3\text{C})_3\text{SiSiH}_3$	1303-1281	1277-1255	$\text{HN}[\text{Si}(\text{NH}_2)_2]_2$	1184	1148	
$\text{H}_2\text{C}[\text{Si}(\text{OH})_2]_2$	1078	1056	$\text{H}_3\text{CSi}(\text{CH}_3)_3$	1299	1273	$\text{HN}[\text{Si}(\text{OH})_2]_2$	1177	1142	
			$\text{H}_3\text{CSi}(\text{NH}_2)_3$	1293	1267				
			$\text{H}_3\text{CSi}(\text{OH})_3$	1305	1279				

containing amorphous materials [44], empirical relations have been established between $\nu(\text{Si—H stretch.})$ and the electronegativity of neighboring atoms. We present here a systematic DFT study of this absorption mode in $\text{SiC}_x\text{N}_y(\text{O})\text{:H}$ materials.

Calculated $\nu(\text{Si—H stretch.})$ in $\text{X}_3\text{—SiH}$, $\text{X}_2\text{—SiH}_2$, X—SiH_3 ($\text{X} = \text{Si, C, N or O}$) are reported in Table 2. DFT confirms the two following trends previously described by Lucovsky [44]:

- For $\text{X} = \text{Si or C}$, $\nu(\text{Si—H stretch.})$ in $\text{X}_3\text{—}_x\text{—SiH}_x$ increases with x , although the opposite behavior is observed for $\text{X} = \text{N or O}$ as $\nu(\text{Si—H stretch.})$ is unchanged or decreases when x increases (dashed line in Fig. 2).
- For a given x , $\nu(\text{Si—H stretch.})$ increases with the electronegativity of X substituents.

The latter point was also discussed in the literature for molecular compounds [43]: for $\text{X}_3\text{Si—H}$ moieties, the $\nu(\text{Si—H stretch.})$ shift toward higher wavenumber within the series $\text{X} = \text{Si, C, N or O}$ is attributed to inductive effects [45]. DFT calculations confirm this hypothesis.

For amorphous materials such as $\text{a-SiC}_x\text{:H}$ [46], $\text{a-SiN}_x\text{:H}$ [47–49] and $\text{a-SiO}_x\text{:H}$ [50], Lucovsky's approach led to the vibration wavenumbers attributions as reported in Table 2. These values are in relatively good agreement with DFT results. Discrepancies can be attributed to several factors. Firstly, limitations arise from the calculation method, e.g. an error of 1% on the scale factor leads to an uncertainty of $\sim 20\text{ cm}^{-1}$ in the $\nu(\text{Si—H stretch.})$ domain. Secondly, low experimental wavenumbers (e.g. $\text{Si}_3\text{—SiH}$ moieties give bands in the range $2000\text{--}2013\text{ cm}^{-1}$ [46]) can be explained by using the Cardona model [51,52]. This model predicts that when Si—H bond is located in a cavity, $\nu(\text{Si—H stretch.})$ decreases with decreasing radius of the cavity. Such a confinement effect has not been taken into account in our calculations. One should note that Cardona model is discussed elsewhere [37].

In the $\text{a-SiC}_x\text{N}_y(\text{O})\text{:H}$ materials, the band in the range $2000\text{--}2220\text{ cm}^{-1}$ has been attributed to $\nu(\text{Si—H stretch.})$ in $\text{X}_3\text{—SiH}$, $\text{X}_2\text{—SiH}_2$, X—SiH_3 moieties (Fig. 1 and references herein). An example is given in Fig. 4 which presents the FTIR spectrum of PECVD $\text{a-SiC}_x\text{N}_y(\text{O})\text{:H}$ thin film deposited from a plasma containing hexamethyldisilazane, NH_3 and Ar [26]. For this material, the maximum of the Si—H stretching absorption band is reported at 2180 cm^{-1} , although DFT calculations yield $\nu(\text{Si—H stretch.})$ below 2135 cm^{-1} (Table 2) for $\text{X}_3\text{—SiH}$, $\text{X}_2\text{—SiH}_2$, X—SiH_3 moieties (with $\text{X} = \text{Si, C or N}$). Then, it appears that these DFT calculations can hardly reproduce the high wavenumber side of the absorption band observed for this material.

At this point three chemical moieties can be considered to account for these wavenumbers, as discussed below.

- Wave numbers values up to $\sim 2220\text{ cm}^{-1}$ corresponding to $\nu(\text{Si—H stretch.})$ are calculated for oxygenated $\text{X}_3\text{—SiH}$,

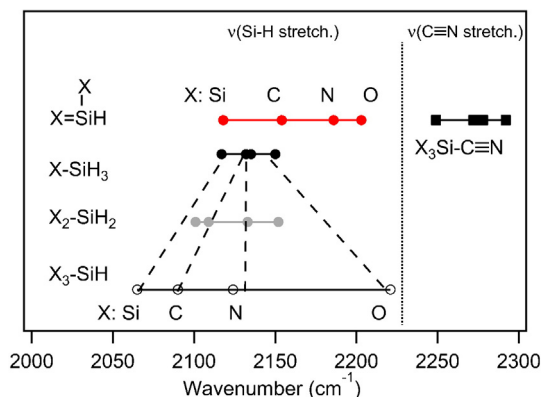


Fig. 2. Positions of $\nu(\text{Si—H stretch.})$ and $\nu(\text{C≡N stretch.})$ absorption bands calculated at DFT B3LYP/6-311++G(3df,3pd) level of theory. Dashed lines are only guides for the eyes.

$\text{X}_2\text{—SiH}_2$, X—SiH_3 moieties (Table 2). Thus, high wavenumber values for $\nu(\text{Si—H stretch.})$ could be the mark for a substantial oxygen pollution of the silicon carbonitride material.

- Calculation for $\text{Si}_{\text{sp}^2}\text{—H}$ moieties give $\nu(\text{Si—H stretch.})$ up to $\sim 2200\text{ cm}^{-1}$ (Table 2). As far as we know, it is worth noticing that such moieties were not previously considered in the $\text{a-SiC}_x\text{N}_y(\text{O})\text{:H}$ materials. In the particular case given in Fig. 4, combined FTIR and XPS study [26] indicate that atomic oxygen content is close to 3%, which rules out the former explanation. On the other hand, DFT calculations of $\nu(\text{Si—H stretch.})$ position in N—SiHN (2186 cm^{-1}) perfectly match with measurements.
- Finally, C≡N stretching was sometimes invoked to explain the upper part of the Si—H stretching feature (Fig. 1). The possible contribution of this vibration mode can be ruled out here, as discussed in the following paragraph.

3.7. C≡N stretching

The position of $\nu(\text{C≡N stretch.})$ absorption band in $\text{SiC}_x\text{N}_y(\text{O})\text{:H}$ was reported to lie in the range $2100\text{--}2300\text{ cm}^{-1}$. As already mentioned above and shown in Fig. 1, there is no clear consensus in the literature regarding the discrimination between $\nu(\text{C≡N stretch.})$ and $\nu(\text{Si—H stretch.})$ which lies in the range $2000\text{--}2220\text{ cm}^{-1}$. DFT calculations in Si—C≡N and C—C≡N give wavenumbers higher than 2249 cm^{-1} , see Table 2. $\nu(\text{C≡N stretch.})$ significantly increases from 2249 cm^{-1} in $\text{Si}_3\text{SiC≡N}$ to 2292 cm^{-1} in $\text{O}_3\text{SiC≡N}$ environment. As detailed below for Si—H stretching mode, this shift results from the enhancement of the nitrile bond when X in $\text{X}_3\text{SiC≡N}$ becomes more electronegative. Then one can expect to observe the bands corresponding to $\nu(\text{Si—H stretch.})$ and $\nu(\text{C≡N stretch.})$ respectively below and above $\sim 2230\text{ cm}^{-1}$ (Fig. 2). Moreover, it should be note that the highest $\nu(\text{Si—H stretch.})$ is obtained for highly oxygenated environment: according to our calculations poorly oxygenated silicon carbonitride would present $\nu(\text{Si—H stretch.})$ below 2186 cm^{-1} . This result will be a valuable guide for an easier identification of Si—H and C≡N moieties in $\text{SiC}_x\text{N}_y(\text{O})\text{:H}$ materials.

3.8. Si—H stretching vs C≡N stretching

In the case of the (low frequency PECVD) $\text{SiC}_x\text{N}_y(\text{O})\text{:H}$ film whose FTIR spectrum is shown in Fig. 4, the absorption band is located, below 2200 cm^{-1} , at 2180 cm^{-1} , which rules out the possible contribution of C≡N moieties. This analysis also confirms the assignment given in [28] for microwave PECVD $\text{SiC}_x\text{N}_y(\text{O})\text{:H}$ films for which the absorption band centered at 2170 cm^{-1} has been attributed to Si—H bond. Upon ageing, this band decays while the Si—O band ($\sim 1040\text{ cm}^{-1}$) increases indicating that Si—H bond are tightly involved in film oxidation. It is worth noticing that calculated frequencies suggest the presence $\text{Si}_{\text{sp}^2}\text{—H}$ bond while Si_{sp^2} can undergo addition reaction. Then, one can infer that the minimization of Si—H bond would enhance the stability of $\text{SiC}_x\text{N}_y(\text{O})\text{:H}$ films.

FTIR spectra of hydrogenated Si—B—C—N films also present an absorption band slightly below 2200 cm^{-1} attributed to Si—H stretching/ C≡N stretching modes [29]. Since boron electronegativity is intermediate between those of Si and C , $\nu(\text{Si—H stretch.})$ frequency in B_3SiH is calculated at 2075 cm^{-1} (unscaled frequency equals 2161 cm^{-1}), i.e. in between calculated $\nu(\text{Si—H stretch.})$ frequencies in Si_3SiH (2065 cm^{-1}) and C_3SiH (2090 cm^{-1}). Similarly, $\nu(\text{C≡N stretch.})$ frequency in B_3SiCN is calculated at 2262 cm^{-1} (unscaled frequency equals 2285 cm^{-1}), i.e. in between calculated $\nu(\text{C≡N stretch.})$ frequencies in Si_3SiCN (2249 cm^{-1}) and C_3SiCN (2292 cm^{-1}). Thus, inductive effect of boron on either $\nu(\text{C≡N stretch.})$ or $\nu(\text{Si—H stretch.})$ cannot account for the position of the absorption band at 2200 cm^{-1} . As for $\text{SiC}_x\text{N}_y(\text{O})\text{:H}$ film, DFT calculations lead to assign this band to $\text{Si}_{\text{sp}^2}\text{—H}$ moieties.

3.9. C—H stretching/N—H stretching

The position of $\nu(\text{C—H stretch.})$ absorption band in $(\text{X}_3\text{Si})_2\text{—CH}_2$ and $\text{X}_3\text{Si—CH}_3$ moieties (with $\text{X} = \text{Si, C, N or O}$) were calculated to lie in the range $2865\text{--}2974\text{ cm}^{-1}$ (Table 2), in good agreement with experimental data (Fig. 1). $\nu(\text{C—H stretch.})$ increases roughly with the electronegativity of substituent X . In $\text{X}_3\text{Si—CH}_3$, this effect is limited: the variation of $\nu(\text{C—H stretch.})$ is less than 0.5% when $\text{X} = \text{Si}$ is replaced by O . Calculations of $\nu(\text{N—H stretch.})$ wavenumbers are more instructive. Indeed, DFT calculations indicate that $(\text{X}_3\text{Si})_2\text{—NH}$ moieties gives rise to one band below 3500 cm^{-1} , while $\text{X}_3\text{Si—NH}_2$ give rise to two bands, respectively, below and above 3500 cm^{-1} (Table 2). This is fully in line with the results published on organosilicon compounds [45] and suggests to reconsider some of the attributions in Fig. 1: in $\text{SiC}_x\text{N}_y(\text{O})\text{:H}$ materials; the absorption band located below 3500 cm^{-1} should be associated solely to NH moieties. Finally $\nu(\text{N—H stretch.})$ increases with the electronegativity of substituent X . This result will be discussed in the next section.

3.10. Frequency shift and chemical environment

As noted above, the vibration frequencies of Si—C , Si—N , Si—H , C—H , N—H and $\text{C}\equiv\text{N}$ stretching modes increase when neighbor atoms become more electronegative. If we first focus on Si—H moieties: Fig. 3 presents 2D maps of the electronic density in $\text{Si}_3\text{Si—H}$ (left) as well as the differences in electronic density between $\text{X}_3\text{Si—H}$ and $\text{Si}_3\text{Si—H}$ (with $\text{X} = \text{C, N or O}$). It clearly appears that the electronic density in the vicinity of a Si atom involved in Si—H bond decreases with increasing electronegativity of substituents. This is accompanied by both a decrease of Si—H bond length (from 1.492 to 1.463 \AA) and an increase of electron density in this bond. Electron transfer from Si to its substituents leads to a rise of the Si—H bond force constant and then of $\nu(\text{Si—H stretch.})$ vibration frequency. In this sense DFT analysis confirms that $\nu(\text{Si—H stretch.})$ shift is due to inductive effect [45]. Similar effect was evidenced for Si—O stretching mode in Si—OH moieties by means of DFT calculations [33]. This analysis can be extended here to Si—C , Si—N , C—H , N—H and $\text{C}\equiv\text{N}$ bonds. It should be noted that the relative variations of both frequency and bond length are correlated. For example, the relative variations of $\nu(\text{Si—N stretch.})$ and Si—N length in $\text{H}_2\text{N—SiX}_3$ when $\text{X} = \text{Si}$ is replaced by O are equal to 19% and 3% respectively. By contrast, the relative variations of $\nu(\text{C—H stretch.})$ and C—H length in $\text{H}_3\text{C—SiX}_3$ when $\text{X} = \text{Si}$ is replaced by O are equal to 0.5% and 0.1%, respectively.

4. Conclusion

A systematic study of the vibrational properties of Si—C , Si—N , $\text{C}\equiv\text{N}$, Si—H , C—H and N—H moieties in hydrogenated silicon carbonitride materials was carried out at DFT B3LYP/6-311++G(3df,3pd) level of theory. In here, main attention was paid to the role of chemical environment on vibration frequencies. It turns

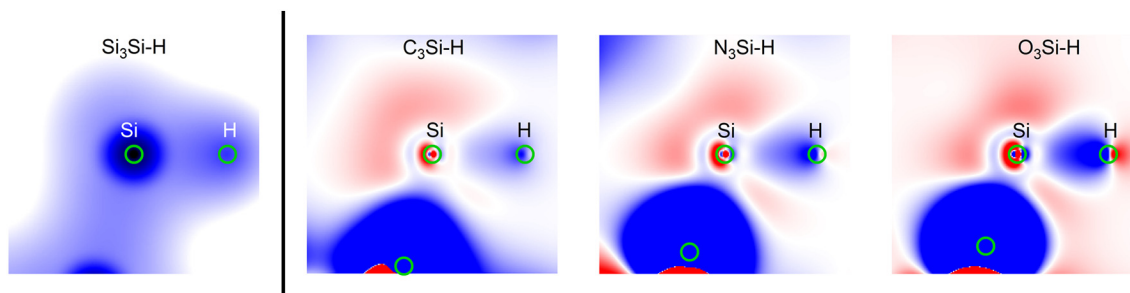


Fig. 3. 2D maps ($4 \times 4\text{ \AA}$) showing the electronic density for $\text{Si}_3\text{Si—H}$ (left) and the differences in electronic density between $\text{X}_3\text{Si—H}$ (with $\text{X} = \text{C, N or O}$) and $\text{Si}_3\text{Si—H}$ moieties (right). Blue and red colors correspond respectively to positive and negative values of the electronic density. Circles are located at atom position. (For interpretation of the references to color in this figure legend, the reader is referred to the web version of this article.)

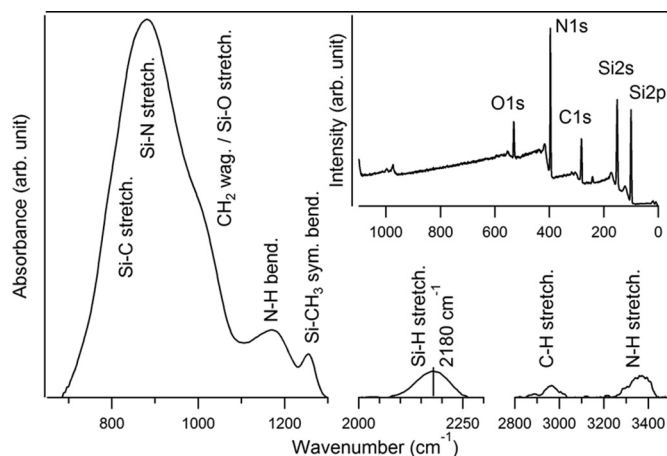


Fig. 4. FTIR spectrum (and X-ray photoemission spectrum, inset) of $\text{a-SiC}_x\text{N}_y(\text{O})\text{:H}$ thin film deposited by PECVD from a plasma containing hexamethyldisilazane, NH_3 and Ar [26].

out, that calculated wavenumbers largely depend on the chemical environment of silicon atoms, as shown in Fig. 1. The most striking example of this is the shift of calculated $\nu(\text{Si—N stretch.})$ in $\text{H}_2\text{N—SiX}_3$ that increases by 169 cm^{-1} when $\text{X} = \text{Si}$ is replaced by O . This mainly explains the wide dispersion in the position of absorption bands reported in literature for an amorphous material such as $\text{a-SiC}_x\text{N}_y(\text{O})\text{:H}$.

Calculations show that stretching mode frequencies of Si—C , Si—N , Si—H , C—H , N—H and $\text{C}\equiv\text{N}$ moieties in $\text{a-SiC}_x\text{N}_y(\text{O})\text{:H}$ increases when the neighboring atoms become more electronegative due to inductive effect. This generalizes previous experimental and theoretical results [33,44] concerning Si—H or Si—O moieties.

Both $\nu(\text{Si—C stretch.})$ and $\nu(\text{Si—N stretch.})$ are greatly reduced when C (respectively, N) is bonded to H atom: then low vibration frequencies are expected for H -rich materials.

The vibration $\nu(\text{N—H bend.})$ and $\nu(\text{Si—CH}_3\text{ sym. bend.})$ are found in rather a narrow frequency range. In Si—CH_3 , vibrational coupling between CH_3 groups leads to a slight spreading of the absorption band. Similar coupling could explain the reported absorption range for N—H bending mode which is wider than what was calculated. The vibration $\nu(\text{CH}_2\text{ wag.})$ is also located in a narrow frequency range but remains difficult to identify due to overlap with Si—N , Si—O and C—N stretching modes.

DFT calculations predict that both Si—H and $\text{C}\equiv\text{N}$ stretching bands are located below and above $\sim 2230\text{ cm}^{-1}$ respectively. It should be noted that $\nu(\text{Si—H stretch.})$ are found above 2200 cm^{-1} only for oxygen-rich material. Moreover, since the absorption band at $2170\text{--}2180\text{ cm}^{-1}$ is in agreement with the position of the Si—H stretching band in N=SiHN (calculated at 2186 cm^{-1}), calculations lead to consider $\text{Si}_{\text{sp}2}\text{—H}$ moieties in $\text{a-SiC}_x\text{N}_y(\text{O})\text{:H}$ materials. The reactivity of such moieties can be suspected to facilitate material oxidation.

The vibration $\nu(\text{C—H stretch})$ marginally shifts depending on the chemical environment. Si-NH moieties gives rise to one N—H stretching band below 3500 cm^{-1} , while Si-NH₂ yields two bands, respectively, below and above 3500 cm^{-1} .

Results of these calculations will be helpful to identify both the chemical moieties and their environment in future investigations on a-SiC_xN_y:H materials but also on materials containing additional elements such as B- or O-doped SiCN-based systems.

References

- [1] L. Barbadillo, F.J. Gómez, M.J. Hernández, J. Piqueras, Nitrogen incorporation in amorphous SiCN layers prepared from electron cyclotron resonance plasmas, *Appl. Phys. A Mater. Sci. Process.* 68 (1999) 603–607, <http://dx.doi.org/10.1007/s003390050948>.
- [2] I. Martín, M. Vetter, A. Orpella, C. Voz, J. Puigdollers, R. Alcubilla, Surface passivation of n-type crystalline Si by plasma-enhanced-chemical-vapor-deposited amorphous SiC_x:H and amorphous SiC_xN_y:H films, *Appl. Phys. Lett.* 81 (2002) 4461–4463, <http://dx.doi.org/10.1063/1.1527230>.
- [3] T.P. Smirnova, A.M. Badalian, L.V. Yakovkina, V.V. Kaichev, V.I. Bukhtiyarov, A.N. Shmakov, I.P. Asanov, V.I. Rachlin, A.N. Fomina, SiCN alloys obtained by remote plasma chemical vapour deposition from novel precursors, *Thin Solid Films* 429 (2003) 144–151, [http://dx.doi.org/10.1016/S0040-6090\(03\)00408-5](http://dx.doi.org/10.1016/S0040-6090(03)00408-5).
- [4] Z. Chen, K. Prasad, C.Y. Li, S.S. Su, D. Gui, P.W. Lu, X. He, S. Balakumar, Characterization and performance of dielectric diffusion barriers for Cu metallization, *Thin Solid Films* 462–463 (2004) 223–226, <http://dx.doi.org/10.1016/j.tsf.2004.05.036>.
- [5] Y.H. Wang, M.R. Moitreyee, R. Kumar, L. Shen, K.Y. Zeng, J.W. Chai, J.S. Pan, A comparative study of low dielectric constant barrier layer, etch stop and hardmask films of hydrogenated amorphous Si-(C, O, N), *Thin Solid Films* 460 (2004) 211–216, <http://dx.doi.org/10.1016/j.tsf.2004.01.055>.
- [6] P. Jedrzejowski, J. Cizek, A. Amassian, J.E. Klemberg-Sapieha, J. Vlcek, L. Martinu, Mechanical and optical properties of hard SiCN coatings prepared by PECVD, *Thin Solid Films* 447–448 (2004) 201–207, [http://dx.doi.org/10.1016/S0040-6090\(03\)01057-5](http://dx.doi.org/10.1016/S0040-6090(03)01057-5).
- [7] M. Vetter, IR-study of a-SiC_x:H and a-SiC_xN_y:H films for c-Si surface passivation, *Thin Solid Films* 451–452 (2004) 340–344, <http://dx.doi.org/10.1016/j.tsf.2003.10.125>.
- [8] I. Ferreira, E. Fortunato, P. Vilarinho, A.S. Viana, A.R. Ramos, E. Alves, R. Martins, Hydrogenated silicon carbon nitride films obtained by HWCVD, PA-HWCVD and PECVD techniques, *J. Non-Cryst. Solids* 352 (2006) 1361–1366, <http://dx.doi.org/10.1016/j.jnoncrysol.2006.02.025>.
- [9] E. Vassallo, A. Cremona, F. Ghezzi, F. Deller, L. Laguardia, G. Ambrosone, U. Coscia, Structural and optical properties of amorphous hydrogenated silicon carbonitride films produced by PECVD, *Appl. Surf. Sci.* 252 (2006) 7993–8000, <http://dx.doi.org/10.1016/j.apsusc.2005.10.017>.
- [10] I. Blaszczyk-Lezak, A.M. Wrobel, M.P.M. Kivitorama, I.J. Vayrynen, A. Tracz, Silicon carbonitride by remote microwave plasma CVD from organosilicon precursor: growth mechanism and structure of resulting Si:C:N films, *Appl. Surf. Sci.* 253 (2007) 7211–7218, <http://dx.doi.org/10.1016/j.apsusc.2007.02.193>.
- [11] A.M. Wrobel, I. Blaszczyk-Lezak, P. Uznanski, B. Glebocki, Remote hydrogen microwave plasma chemical vapor deposition of amorphous silicon carbonitride (a-SiCN) coatings derived from tris(dimethylamino)silane, *Plasma Process. Polym.* 8 (2011) 542–556, <http://dx.doi.org/10.1002/ppap.201000203>.
- [12] R. Di Mundo, F. Palumbo, F. Fracassi, R. d'Agostino, Methylaminosilane fed inductively coupled plasmas for silicon nitride deposition, *Plasma Process. Polym.* 5 (2008) 770–777, <http://dx.doi.org/10.1002/ppap.200800060>.
- [13] W. Kaffrouni, V. Rouessac, A. Julbe, J. Durand, Synthesis of PECVD a-SiC_xN_y:H membranes as molecular sieves for small gas separation, *J. Membr. Sci.* 329 (2009) 130–137, <http://dx.doi.org/10.1016/j.memsci.2008.12.028>.
- [14] V.I. Ivashchenko, O.K. Porada, L.A. Ivashchenko, I.I. Timofeeva, O.K. Sinelnichenko, O.O. Butenko, M.V. Ushakov, L.A. Ushakova, Characteristics of thin plasmachemical silicon carbon nitride films deposited using hexamethyldisilane, *Powder Metall. Met. Ceram.* 48 (2009) 66–72, <http://dx.doi.org/10.1007/s11106-009-9096-9>.
- [15] B. Swatowska, T. Stapinski, Optical and structural characterization of silicon-carbon-nitride thin films for optoelectronics, *Phys. Status Solidi C* 7 (2010) 758–761, <http://dx.doi.org/10.1002/pssc.200982672>.
- [16] Y. Awad, M.A. El Khakani, M. Scarlete, C. Aktik, R. Smirani, N. Camiré, M. Lessard, J. Mouine, Structural analysis of silicon carbon nitride films prepared by vapor transport-chemical vapor deposition, *J. Appl. Phys.* 107 (2010), 033517, <http://dx.doi.org/10.1063/1.3289732>.
- [17] H. Hoche, C. Pusch, R. Riedel, C. Fasel, A. Klein, Properties of SiCN coatings for high temperature applications — comparison of RF-, DC- and HPPMS-sputtering, *Surf. Coat. Technol.* 205 (2010) S21–S27, <http://dx.doi.org/10.1016/j.surfcoat.2010.03.039>.
- [18] Y. Peng, J. Zhou, B. Zhao, X. Tan, Z. Zhang, Structural and optical properties of the SiCN thin films prepared by reactive magnetron sputtering, *Appl. Surf. Sci.* 257 (2011) 4010–4013, <http://dx.doi.org/10.1016/j.apsusc.2010.11.166>.
- [19] S. Bulou, L. Le Brizoual, P. Miska, L. de Pouques, R. Hugon, M. Belmahi, J. Bougdira, The influence of CH₄ addition on composition, structure and optical characteristics of SiCN thin films deposited in a CH₄/N₂/Ar/hexamethyldisilazane microwave plasma, *Thin Solid Films* 520 (2011) 245–250, <http://dx.doi.org/10.1016/j.tsf.2011.07.054>.
- [20] S. Guruvanket, S. Andrie, M. Simon, K.W. Johnson, R.A. Sailer, Atmospheric pressure plasma CVD of amorphous hydrogenated silicon carbonitride (a-SiCN:H) films using triethylsilane and nitrogen, *Plasma Process. Polym.* 8 (2011) 1126–1136, <http://dx.doi.org/10.1002/ppap.201100035>.
- [21] S. Guruvanket, S. Andrie, M. Simon, K.W. Johnson, R.A. Sailer, Atmospheric-pressure plasma-enhanced chemical vapor deposition of a-SiCN:H films: role of precursors on the film growth and properties, *ACS Appl. Mater. Interfaces* 4 (2012) 5293–5299, <http://dx.doi.org/10.1021/am301157p>.
- [22] S. Bulou, L. Le Brizoual, P. Miska, L. de Pouques, J. Bougdira, M. Belmahi, Wide variations of SiC_xN_y:H thin films optical constants deposited by H₂/N₂/Ar/hexamethyldisilazane microwave plasma, *Surf. Coat. Technol.* 208 (2012) 46–50, <http://dx.doi.org/10.1016/j.surfcoat.2012.07.079>.
- [23] S. Peter, S. Bernütz, S. Berg, F. Richter, FTIR analysis of a-SiCN:H films deposited by PECVD, *Vacuum* 98 (2013) 81–87, <http://dx.doi.org/10.1016/j.vacuum.2013.04.014>.
- [24] V. Kulikovskiy, R. Ctvrtlik, V. Vorlicek, V. Zelezny, P. Bohac, L. Jastrabik, Effect of air annealing on mechanical properties and structure of SiC_xN_y magnetron sputtered films, *Surf. Coat. Technol.* 240 (2014) 76–85, <http://dx.doi.org/10.1016/j.surfcoat.2013.12.017>.
- [25] J.A. Silva, S. Quoizola, E. Hernandez, L. Thomas, F. Massines, Silicon carbon nitride films as passivation and antireflective coatings for silicon solar cells, *Surf. Coat. Technol.* 242 (2014) 157–163, <http://dx.doi.org/10.1016/j.surfcoat.2014.01.037>.
- [26] R. Coustel, M. Haacké, V. Rouessac, J. Durand, M. Drobek, A. Julbe, An insight into the structure–property relationships of PECVD SiC_xN_y(O):H materials, *Microporous Mesoporous Mater.* 191 (2014) 97–102, <http://dx.doi.org/10.1016/j.micromeso.2014.02.043>.
- [27] M. Haacké, R. Coustel, V. Rouessac, M. Drobek, S. Rouldès, A. Julbe, Optimization of the molecular sieving properties of amorphous SiC_xN_y:H hydrogen selective membranes prepared by PECVD, *Eur. Phys. J. Spec. Top.* 224 (2015) 1935–1943, <http://dx.doi.org/10.1140/epjst/e2015-02511-y>.
- [28] M. Haacké, R. Coustel, V. Rouessac, S. Rouldès, A. Julbe, Microwave PECVD silicon carbonitride thin films: a FTIR and ellipsosporimetry study: microwave PECVD silicon carbonitride thin films..., *Plasma Process. Polym.* 13 (2016) 258–265, <http://dx.doi.org/10.1002/ppap.201500058>.
- [29] J. Čížek, J. Vlček, Š. Potocký, J. Houška, Z. Soukup, J. Kalaš, P. Jedrzejowski, J.E. Klemberg-Sapieha, L. Martinu, Mechanical and optical properties of quaternary Si–B–C–N films prepared by reactive magnetron sputtering, *Thin Solid Films* 516 (2008) 7286–7293, <http://dx.doi.org/10.1016/j.tsf.2007.12.156>.
- [30] G. Orce, J. Phalippou, L.L. Hench, Structural changes of silica xerogels during low temperature dehydration, *J. Non-Cryst. Solids* 88 (1986) 114–130, [http://dx.doi.org/10.1016/S0022-3093\(86\)80092-8](http://dx.doi.org/10.1016/S0022-3093(86)80092-8).
- [31] R. Al-Oweini, H. El-Rassy, Synthesis and characterization by FTIR spectroscopy of silica aerogels prepared using several Si(OR)₄ and R'Si(OR')₃ precursors, *J. Mol. Struct.* 919 (2009) 140–145, <http://dx.doi.org/10.1016/j.molstruc.2008.08.025>.
- [32] J. Percino, J.A. Pacheco, G. Soriano-Moro, M. Cerón, M.E. Castro, V.M. Chapela, J. Bonilla-Cruz, T.E. Lara-Ceniceros, M. Flores-Guerrero, E. Saldívar-Guerra, Synthesis, characterization and theoretical calculations of model compounds of silanols catalyzed by TEMPO to elucidate the presence of Si–O–Si and Si–O–N bonds, *RSC Adv.* 5 (2015) 79829–79844, <http://dx.doi.org/10.1039/C5RA10056A>.
- [33] C. Carteret, Vibrational properties of silanol group: from alkylsilanol to small silica cluster, *Spectrochim. Acta A Mol. Biomol. Spectrosc.* 64 (2006) 670–680, <http://dx.doi.org/10.1016/j.saa.2005.08.004>.
- [34] C. Carteret, A. Labrosse, X. Assfeld, An ab initio and DFT study of structure and vibrational spectra of disiloxane H₃SiOSiH₃ conformers, *Spectrochim. Acta A Mol. Biomol. Spectrosc.* 67 (2007) 1421–1429, <http://dx.doi.org/10.1016/j.saa.2006.10.041>.
- [35] C. Carteret, A. Labrosse, Vibrational properties of polysiloxanes: from dimer to oligomers and polymers. 1. Structural and vibrational properties of hexamethyldisiloxane (CH₃)₂SiOSi(CH₃)₂, *J. Raman Spectrosc.* 41 (2010) 996–1004, <http://dx.doi.org/10.1002/jrs.2537>.
- [36] A. Alparone, Vibrational and electronic spectra of silole: a theoretical PT2-DFT anharmonic and TD-DFT study, *J. Appl. Spectrosc.* 81 (2014) 320–327, <http://dx.doi.org/10.1002/jas.10812-014-9931-8>.
- [37] A.V. Larin, D.V. Milyaeva, A.A. Rybakov, D.S. Bezrukov, D.N. Trubnikov, Internal (SiH)_x groups, X = 1–4, in microcrystalline hydrogenated silicon and their IR spectra on the basis of periodic DFT modelling, *Mol. Phys.* 112 (2014) 956–962, <http://dx.doi.org/10.1080/00268976.2013.817621>.
- [38] A.D. Becke, Density-functional thermochemistry. III. The role of exact exchange, *J. Chem. Phys.* 98 (1993) 5648–5652, <http://dx.doi.org/10.1063/1.464913>.
- [39] C. Lee, W. Yang, R.G. Parr, Development of the Colle-Salvetti correlation-energy formula into a functional of the electron density, *Phys. Rev. B* 37 (1988) 785–789, <http://dx.doi.org/10.1103/PhysRevB.37.785>.
- [40] M.W. Schmidt, K.K. Baldridge, J.A. Boatz, S.T. Elbert, M.S. Gordon, J.H. Jensen, S. Koseki, N. Matsunaga, K.A. Nguyen, S. Su, T.L. Windus, M. Dupuis, J.A. Montgomery, General atomic and molecular electronic structure system, *J. Comput. Chem.* 14 (1993) 1347–1363, <http://dx.doi.org/10.1002/jcc.540141112>.
- [41] K. Yagi, K. Hirao, T. Taketsugu, M.W. Schmidt, M.S. Gordon, Ab initio vibrational state calculations with a quartic force field: applications to H[sub 2]CO, C[sub 2]H[sub 2], CH[sub 3]OH, CH[sub 3]CCH, and C[sub 2]H[sub 6], *J. Chem. Phys.* 121 (2004) 1383–1389, <http://dx.doi.org/10.1063/1.1764501>.
- [42] J.P. Merrick, D. Moran, L. Radom, An evaluation of harmonic vibrational frequency scale factors, *J. Phys. Chem. A* 111 (2007) 11683–11700, <http://dx.doi.org/10.1021/jp073974n>.
- [43] A.L. Smith, N.C. Angelotti, Correlation of the SiH stretching frequency with molecular structure, *Spectrochim. Acta* 15 (1959) 412–420, [http://dx.doi.org/10.1016/S0371-1951\(59\)80334-9](http://dx.doi.org/10.1016/S0371-1951(59)80334-9).
- [44] G. Lucovsky, Chemical effects on the frequencies of Si-H vibrations in amorphous solids, *Solid State Commun.* 29 (1979) 571–576, [http://dx.doi.org/10.1016/0038-1098\(79\)90666-5](http://dx.doi.org/10.1016/0038-1098(79)90666-5).

- [45] N.B. Colthup, L.H. Daly, S.E. Wiberley, *Introduction to Infrared and Raman Spectroscopy*, 3rd ed. Academic Press, Boston, 1990.
- [46] E. Gat, M.A. El Khakani, M. Chaker, A. Jean, S. Boily, H. Pépin, J.C. Kieffer, J. Durand, B. Cros, F. Rousseaux, S. Gujrathi, A study of the effect of composition on the microstructural evolution of a-Si_xC_{1-x}:H PECVD films: IR absorption and XPS characterizations, *J. Mater. Res.* 7 (1992) 2478–2487, <http://dx.doi.org/10.1557/JMR.1992.2478>.
- [47] E. Bustarret, M. Bensouda, M.C. Habrard, J.C. Bruyère, S. Poulin, S.C. Gujrathi, Configurational statistics in a-Si_xNyHz alloys: a quantitative bonding analysis, *Phys. Rev. B* 38 (1988) 8171–8184, <http://dx.doi.org/10.1103/PhysRevB.38.8171>.
- [48] S.-Y. Lin, Electronic and vibrational properties of hydrogenated amorphous silicon nitride, *J. Optoelectron. Adv. Mater.* 4 (2002) 543–552.
- [49] F. Giorgis, F. Giuliani, C.F. Pirri, E. Tresso, C. Summonte, R. Rizzoli, R. Galloni, A. Desalvo, P. Rava, Optical, structural and electrical properties of device-quality hydrogenated amorphous silicon-nitrogen films deposited by plasma-enhanced chemical vapour deposition, *Philos. Mag. B* 77 (1998) 925–944, <http://dx.doi.org/10.1080/13642819808206395>.
- [50] W.K. Chang, M.Y. Liao, K.K. Gleason, Characterization of porous silicon by solid-state nuclear magnetic resonance, *J. Phys. Chem.* 100 (1996) 19653–19658, <http://dx.doi.org/10.1021/jp961921s>.
- [51] H. Wieder, M. Cardona, C.R. Guarnieri, Vibrational spectrum of hydrogenated amorphous Si-C films, *Phys. Status Solidi B* 92 (1979) 99–112, <http://dx.doi.org/10.1002/pssb.2220920112>.
- [52] M. Cardona, Vibrational spectra of hydrogen in silicon and germanium, *Phys. Status Solidi B* 118 (1983) 463–481, <http://dx.doi.org/10.1002/pssb.2221180202>.